Journal of Organometallic Chemistry 696 (2011) 235–243

Contents lists available at ScienceDirect

Journal of Organometallic Chemistry

journal homepage: www.elsevier.com/locate/jorganchem

Understanding the role of an easy-to-prepare aldimine–alkyne carboamination catalyst, $[Ti(NMe_2)_3(NHMe_2)][B(C_6F_5)_4]$

Falguni Basuli, Benjamin Wicker, John C. Huffman, Daniel J. Mindiola*

Department of Chemistry and Molecular Structure Center, Indiana University, Bloomington, IN 47405, USA

ARTICLE INFO

Article history:
Received 4 August 2010
Received in revised form
2 September 2010
Accepted 3 September 2010
Available online 21 September 2010

Keywords:
Carboamination
Titanium
Imido
Nitrogen

ABSTRACT

A series of reactivity studies of the carboamination pre-catalyst $[Ti(NMe_2)_3(NHMe_2)][B(C_6F_5)_4]$ as well as the preparation of other catalysts are reported in this work. Treatment of $[Ti(NMe_2)_3(NHMe_2)][B(C_6F_5)_4]$ with the aldimines Ar′N=CHtol (Ar′ = 2,6-$Me_2C_6H_3$, tol = 4-MeC_6H_4), and depending on the reaction conditions, results in isolation of $[Me_2N{=}CHR'][B(C_6F_5)_4]$ (**1**) or $(Me_2N)_2$CHtol, as well as the asymmetric titanium dimer $[(Me_2N)_2(HNMe_2)Ti(\mu_2\text{-}N[2,6\text{-}Me_2C_6H_3])_2Ti(NHMe_2)(NMe_2)][B(C_6F_5)_4]$ (**2**). Protonation of $CpTi(NMe_2)_3$ and $Cp^*Ti(NMe_2)_3$ results in isolation of the salts, $[CpTi(NMe_2)_2(NHMe_2)][B(C_6F_5)_4]$ (**3**) and $[Cp^*Ti(NMe_2)_2(NHMe_2)][B(C_6F_5)_4]$ (**4**), respectively. Treatment of compounds **3** or **4** with $H_2N[2,6\text{-}^iPr_2C_6H_3]$ results in formation of the imido salts $[CpTi(=N[2,6\text{-}^iPr_2C_6H_3])(NHMe_2)_2][B(C_6F_5)_4]$ (**5**) (58% yield) or $[Cp^*Ti(=N[2,6\text{-}^iPr_2C_6H_3])(NHMe_2)_2][B(C_6F_5)_4]$ (**6**). When $Ti(NMe_2)_4$ is treated with $[Et_3Si][B(C_6F_5)_4]$, the salt $[Ti(NMe_2)_3(N[SiEt_3]Me_2)][B(C_6F_5)_4]$ (**7**) is obtained, and treatment of the latter with $[2,6\text{-}^iPr_2C_6H_3]N{=}$CHtol produces the imine adduct $[Ti(NMe_2)_3(\kappa^1\text{-}[2,6\text{-}^iPr_2C_6H_3]N{=}CHtol)][B(C_6F_5)_4]$ (**8**). The carboamination catalytic activity of complexes **2**–**7** was investigated and compared to $[Ti(NMe_2)_3(NHMe_2)][B(C_6F_5)_4]$. Likewise, a proposed mechanism to the active carboamination catalyst stemming from $[Ti(NMe_2)_3(NHMe_2)][B(C_6F_5)_4]$ is described.

1. Introduction

In 2004 the Bergman group discovered a catalytic reaction where an aldimine can be added across an internal alkyne to form an α,β-unsaturated imine (denoted as the carboamination of alkynes with aldimines, Scheme 1) [1,2]. This interesting transformation was made possible via the use of a transient, mononuclear zirconocene imido precursor, $[Cp_2Zr{=}NAr]$ (Ar = *p*-substituted aryl where the *p*-group is H, OMe, or Me), which could reversibly [2 + 2]-cycloadd the alkyne, then insert the aldimine into the Zr–C bond of the aza-metallacyclobutene species (Scheme 1) [1,2]. A [4 + 2] retro-cycloaddition stemming from the six-membered metallacycle resulted in extrusion of α,β-unsaturated imine concurrent with regeneration of the imido thereby closing the cycle for carboamination of alkynes with aldimines (Scheme 1). Cleverly, the Bergman system applied a zirconium pre-catalyst $Cp_2Zr(NHAr)(CH_3)$ (or the corresponding metallacyclobutene complex resulting from [2 + 2]-cycloaddition of the alkyne across the Zr=N bond of $[Cp_2Zr{=}NAr]$), which underwent thermolytic α-hydrogen abstraction to generate the transient imide, $[Cp_2Zr{=}NAr]$. In the absence of the alkyne such an intermediate would dimerize thereby killing its catalytic activity. Despite this attractive entry to these new organic frameworks, typical reaction conditions involving the metallocene system required extensive time frames, high temperatures using 10–20 mol% of catalyst, as well as the system had also limited range of functional group tolerance at both the aldimine and alkyne substrates [2]. The reaction also suffered from not being atom-economical when the imido group on zirconium was inequivalent to the aldimine *N*-aryl group given the ability of $[Cp_2Zr{=}NAr]$ to undergo imine metathesis with the aldimine and hence afford a mixture of α,β-unsaturated imines when $R^2 \neq R^1$ (Scheme 1) [3]. This was the consequence of having a mixture of $[Cp_2Zr{=}NAr]$ catalysts which would unavoidably result in two separate cycles therefore lowering the yield of the unsaturated organic product.

In an attempt to circumvent some of these limitations, and given our interest in the reactivity and the catalytic ability of 3d early-transition metal complexes having metal-ligand multiple bonds [4,5], we explored the role of various titanium imidos [6–9] in this interesting reaction given the fact that N–C and C–C bonds are catalytically formed and broken. In this contribution we report some investigations toward understanding the role of an easy-to-prepare carboamination pre-catalyst, $[Ti(NMe_2)_3(NHMe_2)][B(C_6F_5)_4]$ [9], by examining the source and role of the imide, variance of the dimethylamide ancillary ligand, and anion or activator being used in the catalytic process.

* Corresponding author. Fax: +1 812 855 8300.
E-mail address: mindiola@indiana.edu (D.J. Mindiola).

0022-328X/$ – see front matter © 2010 Elsevier B.V. All rights reserved.
doi:10.1016/j.jorganchem.2010.09.017

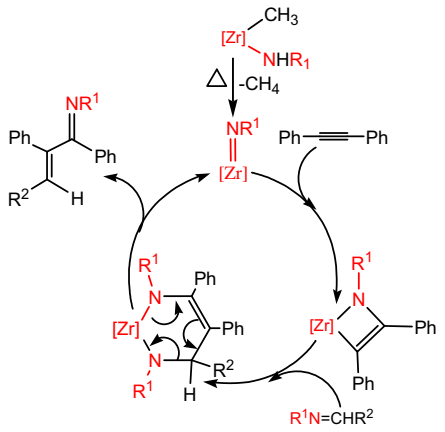

Scheme 1. Proposed Carboamination Cycle Using a Zirconium-Imide Precursor [Zr] = Cp_2Zr.

2. Results and discussion

2.1. Understanding the source of the imide using the carboamination pre-catalyst $[Ti(NMe_2)_3(NHMe_2)][B(C_6F_5)_4]$

We reported previously that mixing of the commercially available reagents $Ti(NMe_2)_4$ with $[NHMe_2Ph][B(C_6F_5)_4]$ gives rise to the salt, $[Ti(NMe_2)_3(NHMe_2)][B(C_6F_5)_4]$, which has been demonstrated to be a very reactive pre-catalyst for the carboamination of alkynes with aldimines [9]. It was found that neither the anilinium proton source nor the neutral titanium complex, alone, were active catalysts for this transformation, which was surprising given that $Ti(NMe_2)_4$ has been shown by Odom and Schafer to be a highly active hydroamination catalyst [10–12]. One peculiar feature of this reaction that we found intriguing was the source of the imide ligand during the carboamination process. It was determined that the absence of aniline, which was presumed to be the source of imido, had no effect in the catalytic formation of the α,β-unsaturated imine [9]. This was puzzling since it is generally accepted that a terminal imido ligand is being transferred in the catalytic cycle (Scheme 1, vide supra) [4,13,14]. The fact that a catalytic carboamination process could occur in the absence of aniline suggested that the imide group is derived from the aldimine as opposed to the aniline. Therefore, we investigated another mechanism to formation of the imide which did not involve the more common route, such as transimination (imide formation derived from aniline deprotonation) [4].

It has been reported that aldimines can serve as an imido source in the presence of suitable nucleophiles [15]. Accordingly, we explored the reactivity of $[Ti(NMe_2)_3(NHMe_2)][B(C_6F_5)_4]$ with aldimines such as Ar′N=CHtol (Ar′ = 2,6-$Me_2C_6H_3$, tol = 4-MeC_6H_4) (Scheme 2) in the absence of diphenylacetylene. Although the reaction yielded a mixture of products after 3 days at 25 °C, we were able to isolate, in low yield, the iminium salt, $[Me_2N{=}CHR'][B(C_6F_5)_4]$ (**1**) (Scheme 2). A single crystal X-ray structure, NMR spectroscopic data and combustion analysis confirmed the proposed connectivity of **1** (Fig. 1)-see Supplementary material. This result therefore suggested that the "NAr" motif of the imine serves as the imido source via the substitution of one $-NMe_2$ ligand in $[Ti(NMe_2)_3(NHMe_2)][B(C_6F_5)_4]$. The most notable structural feature of **1** (Fig. 1) is formation of an iminium motif (N=C, 1.307(6) Å versus N–C bonds of 1.466(5) and 1.470(6) Å), consequently resulting in formation of a planar nitrogen (sum of C–N–C angles = 360°). The reaction depicted in Scheme 2 implies that a neutral, four-coordinate titanium imido, $[ArN{=}Ti(NMe_2)_2(NHMe_2)]$ (**A**), is likely generated in the reaction mixture along with other side products (Scheme 2), although we have no spectroscopic evidence for formation of **A** given the complexity of the mixture. Likewise, attempted synthesis of putative **A** from reactions such as $Ti(NMe_2)_4$ and various anilines failed to produce any isolable product(s) given the lipophilic nature of the complexes being formed.

We, however, argue against **A** being the active catalyst in the carboamination cycle since $Ti(NMe_2)_4$ fails to catalyze the carboamination of alkynes with aldimines in the presence or absence of aniline [9]. Therefore, we propose compound **1** and putative **A** to be formed early in the reaction, but then react to form what we speculate to be the active form of the catalyst. Our hypothesis is in part, corroborated by an independent reaction using similar conditions to those of the catalytic reaction (thermolyzing the mixture). Accordingly, treating tolN=CHtol or [2,6-$Me_2C_6H_3$]N=CHtol with 1 eq. of $[Ti(NMe_2)_3(NHMe_2)][B(C_6F_5)_4]$ in the absence of the alkyne, and then heating the mixture for 5 days at 25 °C afforded a mixture of products from which the organic side product, $(Me_2N)_2CHtol$ could be observed by ^1H NMR spectroscopy and MS analysis as well as comparison with an independently prepared sample [16]. Although we were unable to characterize any titanium products from the reaction involving tolN=CHtol and $[Ti(NMe_2)_3(NHMe_2)][B(C_6F_5)_4]$, the use of a more hindered aldimine, [2,6-$Me_2C_6H_3$]N=CHtol, allowed for isolation of one titanium product. In this case, small quantities of a titanium complex were obtained by fractional crystallization of the reaction mixture from a solution of C_6H_5F layered with hexane. The ^1H NMR spectrum of these crystals revealed formation of an asymmetric complex due to the observation of broad and inequivalent $-NMe_2$ and $-NHMe_2$ resonances. Single crystal structural analysis confirmed this compound to be the imido titanium dimer, $[(Me_2N)_2(HNMe_2)Ti(\mu_2\text{-}N[2,6\text{-}Me_2C_6H_3])_2Ti(NHMe_2)(NMe_2)][B(C_6F_5)_4]$ (**2**) (Fig. 2)-see Supplementary material.

The molecular structure of **2** displays several interesting features such as formation of an asymmetric Ti_2N_2 core (Ti1–N3, 1.800(3); Ti1–N12, 1.877(3); N3–Ti1–N12, 92.93(12); N3–Ti2–N12, 78.49(10); Ti1–N3–Ti2, 92.60(11); Ti1–N12–Ti2, 95.77(11)) due to the bridging of two imido ligands to inequivalent metal centers. These imide groups are most likely derived from the aldimine [2,6-$Me_2C_6H_3$]N=CHtol. As

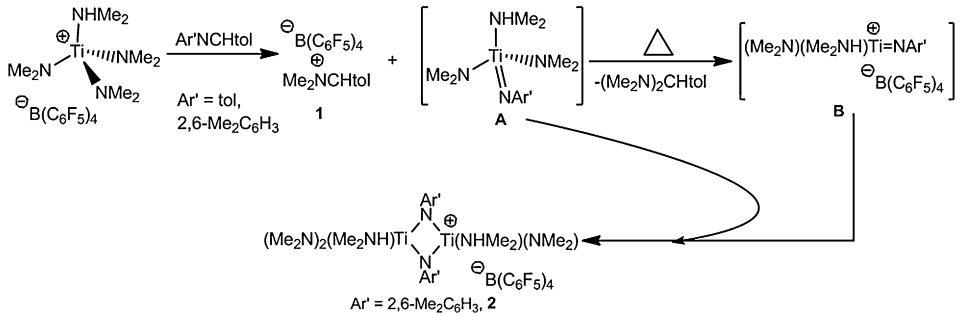

Scheme 2. Proposed route to formation of compound **1** and the titanium complex **2**.

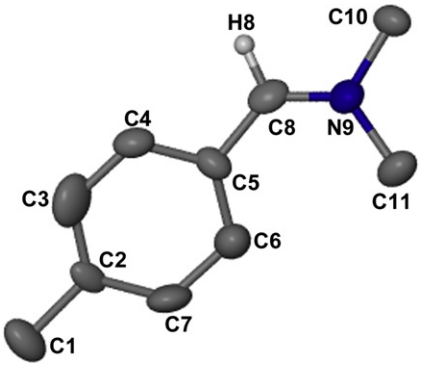

Fig. 1. Molecular structure of compound **1** with thermal ellipsoids at the 50% probability level and with hydrogen atoms (except for the hydrogen on C8), and $B(C_6F_5)_4$ counter anion omitted for the purpose of clarity. Distances are reported in angstroms (Å) and angles in (°). C8–N9, 1.307(6); N9–C10, 1.466(5); N9–C11, 1.470(6); C8–C5, 1.435(4); C8–N9–C10, 120.6(4); C8–N9–C11, 125.4(4); C10–N9–C11, 114.0(4); N9–C8–C5, 129.6(4).

noted, the Ti_2N_2 core is asymmetric due to one titanium center being 5-coordinate, while the other metal center is 4-coordinate and cationic. Formation of a monocation complex having two inequivalent titanium centers, **2**, suggests that the reaction shown in Scheme 2 is likely taking place- transient $(Me_2N)_2Ti{=}NAr$ (**A**) (Ar′ = [2,6-$Me_2C_6H_3$]) dimerizes with an unsaturated titanium imide salt $[(Me_2N)(Me_2NH)Ti{=}N[2,6\text{-}Me_2C_6H_3]][B(C_6F_5)_4]$ (**B**). Formation of transient **B**, or a saturated version coordinated by neutral ligands such as $NHMe_2$ or aldimine, would be consistent with the reaction of **1** with **A** to generate **B** and $(Me_2N)_2$CHtol, which we have observed.

Notably, complex **2** is a highly active carboamination catalyst (125 ° C for 24 h, 90% isolated yield of product when using tolN=CHtol and PhCCPh as substrates), and comparable to the parent precursor complex $[Ti(NMe_2)_3(NHMe_2)][B(C_6F_5)_4]$. These results and observations lend credence to us proposing the following processes taking effect during the carboamination cycle: i) hypothetical three-coordinate (or other masked forms of low-coordinates species) titanium imides and bridging imide salts playing a critical role in the carboamination cycle, ii) aldimine is an effective imide transfer source to $[Ti(NMe_2)_3(NHMe_2)][B(C_6F_5)_4]$, and iii) the dimethylamides are "non-innocent" supporting ligands. Unfortunately, the loss of dimethylamide in the form of $(Me_2N)_2$CHtol implies a non-economical carboamination reaction, and since the supporting dimethylamide ligands are sacrificed during the formation of the active species, this catalyst could die over time.

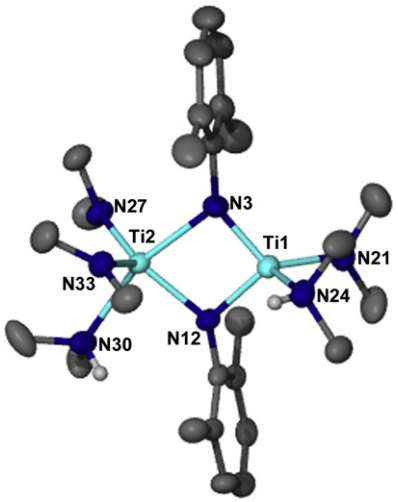

Fig. 2. Molecular structure of complex **2** with thermal ellipsoids at the 50% probability level and with hydrogen atoms (except for the hydrogen on N30 and N24), and one B$(C_6F_5)_4$ counter anion omitted for the purpose of clarity. Four disordered C_6H_5F solvent molecules (two of which lie on center of inversion) have been also omitted. All non-solvent non-hydrogen atoms were refined with anisotropic displacement parameters. Distances are reported in angstroms (Å) and angles in (°). Ti1–Ti2, 2.8942(9); Ti1–N3, 1.800(3); Ti1–N12, 1.877(3); Ti1–N21, 1.900(3); Ti1–N24, 2.157(3); Ti2–N3, 2.186(3); Ti2–N12, 2.023(3); Ti2–N27, 1.884(3); Ti2–N30, 2.274(3); Ti2–N33, 1.908(3); Ti1–N3–Ti2, 92.60(11); Ti1–N12–Ti2, 95.77(11); N3–Ti1–N12, 92.93(12); N3–Ti2–N12, 78.49(10); N21–Ti1–N24, 98.86(14); N3–Ti1–N21, 121.85(14); N3–Ti1–N24, 108.82(12); N3–Ti2–N30, 161.66(11); N3–Ti2–N33, 98.49(12); N3–Ti2–N27, 99.85(12); N24–Ti1–N12, 110.06(12); N21–Ti1–N12, 124.11(13); N12–Ti2–N27, 128.96(12); N12–Ti2–N30, 83.19(11); N12–Ti2–N33, 117.31(12).

2.2. Exploring other ancillary ligands

In addition to $Ti(NMe_2)_4$ we have expanded this study to the monocyclopentadienyl family, namely the known complexes $CpTi(NMe_2)_3$ [18], and $Cp^*Ti(NMe_2)_3$ [19]. Since we have observed that $-NMe_2$ is necessary for incorporation of the imide group, we inquired whether a robust ligand, such as Cp^- or Cp^{*-}, would block this decomposition route and/or result in formation of a more active catalyst. Stoichiometric reactions between the precursors $CpTi(NMe_2)_3$ and $Cp^*Ti(NMe_2)_3$ and $[NHMe_2Ph][B(C_6F_5)_4]$ resulted in formation of the discrete salts $[CpTi(NMe_2)_2(NHMe_2)][B(C_6F_5)_4]$ (**3**) and $[Cp^*Ti(NMe_2)_2(NHMe_2)][B(C_6F_5)_4]$ (**4**), respectively (Scheme 4). We were able to obtain single crystal X-ray diffraction data for each complex (Fig. 3), and we propose that these complexes are formed analogously to the original pre-catalyst, $[Ti(NMe_2)_3(NHMe_2)][B(C_6F_5)_4]$ [9]- protonation of one of the amide ligands without amine loss.

The molecular structure of complex **3** reveals a three-legged piano stool species with one of the amides being protonated see Supplementary material. As a result, the distances between the two amide ligands and titanium (1.8917(17) and 1.8773(17) Å) versus the amine and titanium (2.1992(17) Å) are distinct. The structure of **3** also reveals formation of a discrete salt because of the protonation of only one of the amide ligands. The molecular structure of complex **4** is akin to **3** (see Supplementary material), although it displays a more sterically congested titanium center due to the bulkier Cp^{*-} ligand which is manifested by the longer Ti–Cp (centroid) distance inasmuch as Ti–N distances and more acute N–Ti–N angles (100.90(7), 104.26(7) and 107.75(8)° for **3** versus 98.75(8), 100.41(8) and 105.09(8)° for **4**). The molecular structure of **4** was solved with two independent molecules per asymmetric unit. Instead of isolating complexes **3** and **4**, they can also be

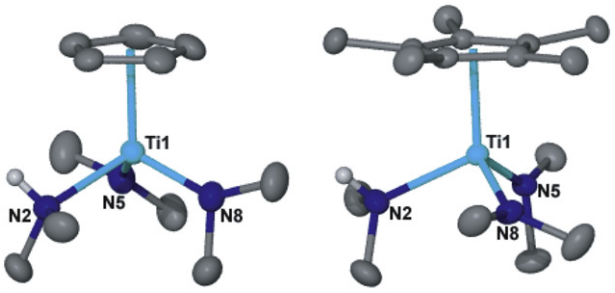

Fig. 3. Molecular structures of complexes **3** (left) and **4** with thermal ellipsoids at the 50% probability level and with hydrogen atoms (except for the hydrogen on N2) omitted for the purpose of clarity. The B$(C_6F_5)_4$ counter anion, one solvent molecule (for **3**), and one of the two crystallographically independent molecules shown for the structure of **4** have been also omitted for the purpose of clarity. Distances are reported in angstroms (Å) and angles in (°). For **3**: Ti1–N2, 2.1992(17); Ti1–N5, 1.8917(17); Ti1–N8, 1.8773(17); Ti1–C(Cp^*), (22.341(2), 2.343(2), 2.365(2), 2.391(2), 2.392(2)); N2–Ti1–N5, 100.90(7); N2–Ti1–N8, 104.26(7); N5–Ti1–N8, 107.75(8). For **4**: Ti1–N2, 2.204(2); Ti1–N5, 1.8969(17); Ti1–N8, 1.8983(18); Ti1–C(Cp^*), (2.340(2), 2.378(2), 2.379(2), 2.411(2), 2.432(2)); N2–Ti1–N5, 98.75(8); N2–Ti1–N8, 100.41(8); N5–Ti1–N8, 105.09(8).

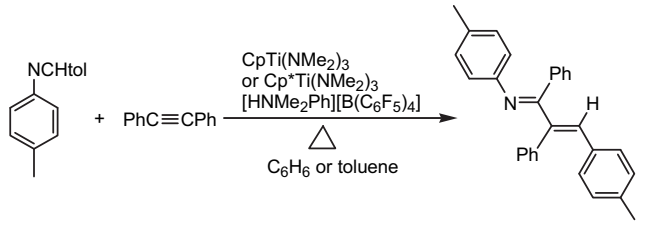

Scheme 3. Catalytic carboamination reactions using monocyclopentadienyl based precursors.

generated *in situ* during the catalytic reaction. Accordingly, protonation of $CpTi(NMe_2)_3$ (10 mol%) with $[NHMe_2Ph][B(C_6F_5)_4]$ (10 mol%) in the presence of diphenylacetylene and the aldimine tolN=CHtol affords the corresponding α,β-unsaturated imine (<40% yields) after 16 h at 130 °C (Scheme 3). As observed with $Ti(NMe_2)_4$, the use of aniline (H_2Ntol) does not affect the outcome of the reaction, implying that the imide, again, is derived from the aldimine. Using the more sterically encumbered precursor $Cp^*Ti(NMe_2)_3$ under the same reaction conditions did not improve reactivity, indicating that neither reagent is as active as the original pre-catalyst $[Ti(NMe_2)_3(NHMe_2)][B(C_6F_5)_4]$ [9].

To establish if the aldimine also undergoes imide group transfer to complexes **3** or **4**, stoichiometric reactions were performed between these complexes and various aldimines, such as ArN=CHtol (Ar = 2,6-$Me_2C_6H_3$, 2,6-$^iPr_2C_6H_3$, tol), over several days at 25 °C. Unfortunately, no products could be isolated from the complicated mixture, so an independent route to the imido was developed. Previous work by our group demonstrated that $Ti(NMe_2)_4$ in the presence of stoichiometric $[NHMe_2Ph][B(C_6F_5)_4]$ and aniline, $H_2N[2,6\text{-}^iPr_2C_6H_3]$, can yield the corresponding imido salt $[Ti(=N2,6\text{-}^iPr_2C_6H_3)(NHMe_2)_3(NMe_2)][B(C_6F_5)_4]$ [9]. Analogously, treating **3** or **4** with $H_2N[2,6\text{-}^iPr_2C_6H_3]$ afforded the corresponding imido complexes, $[CpTi(=N2,6\text{-}^iPr_2C_6H_3)(NHMe_2)_2][B(C_6F_5)_4]$ (**5**) (58% yield) or $[Cp^*Ti(=N2,6\text{-}^iPr_2C_6H_3)(NHMe_2)_2][B(C_6F_5)_4]$ (**6**) (35% yield), respectively (Scheme 4). The ^{1}H NMR spectra of **5** and **6** reveals a freely rotating aryl group on the imido ligand as well as a single environment for the cyclopentadienyl ligand. To conclusively establish the connectivity of these complexes, we collected single crystal structural data on complex **6** (Fig. 4). The molecular structure of **6** reveals a cationic, monomeric titanium imido complex. The Ti=N distance of 1.7309(15) Å and T=N–C_{ipso} angle (162.61(14)°) is consistent with metal-imide formation and is much shorter than the Ti–N_{amine} (2.2011(17) and 2.2178 (17) Å) distances. To avoid clashing with the Cp^* methyl groups the aryl-imide group is almost oriented co-parallel to the Cp^* plane (Fig. 4). The molecular structure of complex **6** resembles previously reported monocyclopentadienyl imido derivatives of titanium [20]. Performing catalytic reactions with **5** or **6** using identical conditions to that reported for $[Ti(NMe_2)_3(NHMe_2)][B(C_6F_5)_4]$ yielded similar results to those observed for precursors $Cp^*Ti(NMe_2)_3$ or $Cp^*Ti(NMe_2)_3$ (vide supra). The fact that the substitution of $-NMe_2$ for a more robust Cp^- or Cp^{*-} ligand lowers the activity of the catalysts is surprising given that monocyclopentadienyl complexes of titanium have been demonstrated to be efficient hydroamination catalysts [20]. Consequently, we propose that the more saturated and sterically protected nature of the **3** and **4** presumably disfavors the cycloaddition or the subsequent insertion step during the carboamination cycle. We argue that the difficult step is not imide formation, as neither the addition of aniline nor the use of the imido complexes improved the catalytic reaction.

2.3. Understanding the role of the activator, $[NHMe_2Ph][B(C_6F_5)_4]$

Our work has established that $[NHMe_2Ph][B(C_6F_5)_4]$ protonates one of the $-NMe_2$ ligands of $Ti(NMe_2)_4$ to yield the discrete salt, $[Ti(NMe_2)_3(NHMe_2)][B(C_6F_5)_4]$ [9]. Very likely, the generation of an amine ligand, $HNMe_2$, is necessary to allow the binding of the substrate, such as an aldimine (vide supra). As a result, we inquired if other "activators" would enhance the reactivity of $Ti(NMe_2)_4$ for the carboamination of alkynes with aldimines. Accordingly, treatment of $Ti(NMe_2)_4$ with $[Et_3Si][B(C_6F_5)_4]$ [21] resulted in the formation of a new complex, $[Ti(NMe_2)_3(N[SiEt_3]Me_2)][B(C_6F_5)_4]$ (**7**) (Scheme 5). Single crystal X-ray diffraction studies of complex **7** confirmed the proposed connectivity as a discrete salt (Fig. 5),

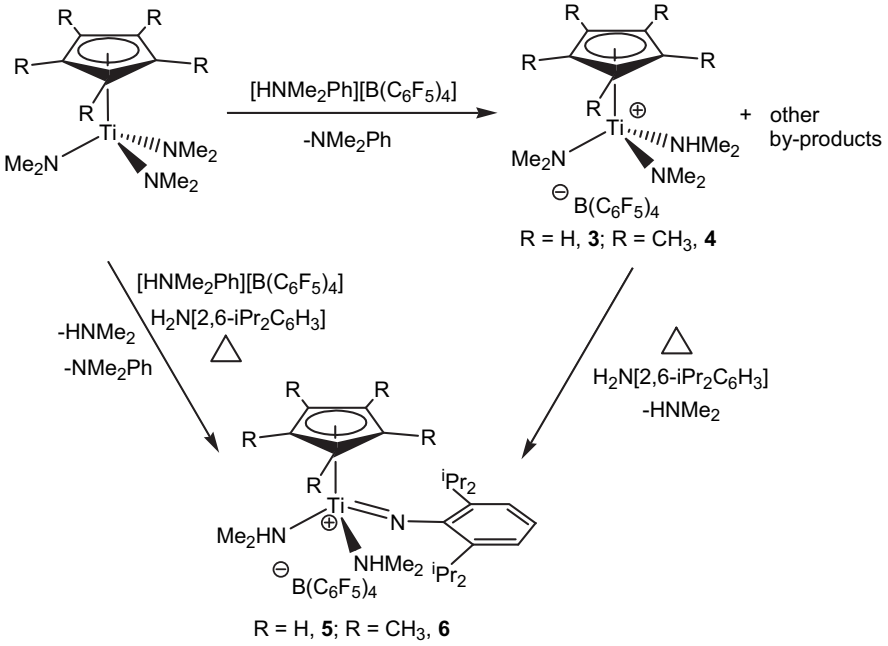

Scheme 4. Synthesis of the salt complexes **3** and **4** and imido complexes **5** and **6**.

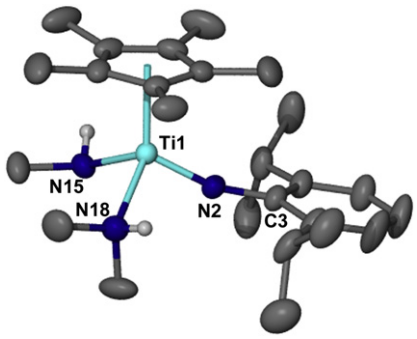

Fig. 4. Molecular structures of complexes **6** with thermal ellipsoids at the 50% probability level and with hydrogen atoms (except for the hydrogen on N15 and N18) omitted for the purpose of clarity. The $B(C_6F_5)_4$ counter anion has been also omitted for the purpose of clarity. Distances are reported in angstroms (Å) and angles in (°). Ti1–N2, 1.7309(15); Ti1–N15, 2.2011(17); Ti1–N18, 2.2178(17); Ti1–C(Cp^*), (2.3349 (19), 2.353(2), 2.3669(18), 2.429(2), 2.4530(19)); N2–Ti1–N15, 103.86(7); N2–Ti1–N18, 97.92(7); N15–Ti1–N18, 100.08(7), Ti1–N2–C3, 162.61(14).

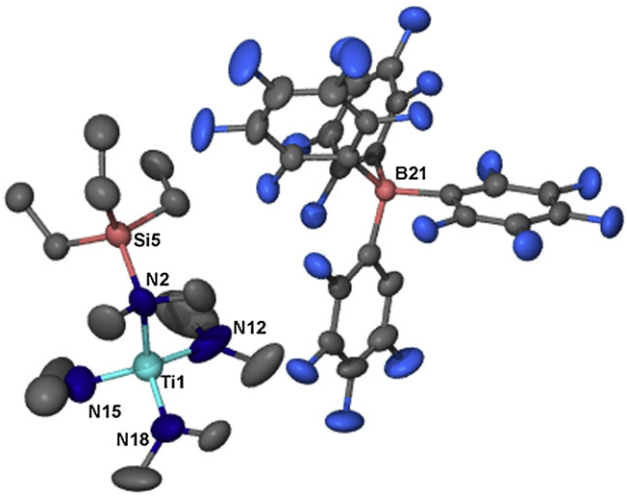

Fig. 5. Molecular structures of complex **7** with thermal ellipsoids at the 50% probability level and with hydrogen atoms omitted for the purpose of clarity. Distances are reported in angstroms (Å) and angles in (°). Ti1–N2, 2.032(5); Ti1–N12, 2.018(9); Ti1–N15, 1.842(7); Ti1–N18, 1.796(9); Si5–N2, 1.844(4); N2–Ti1–N12, 102.1(3); N2–Ti1–N18, 113.4(3); N2–Ti1–N15, 101.2(4); Si5–N2–Ti1, 122.2(2); N12–Ti1–N18, 107.2(3); N12–Ti1–N15, 123.4(3); N18–Ti1–N15, 101.2(4).

formed via the coordination of the $SiEt_3$ cation to the lone pair of electrons in one of the $-NMe_2$ ligand - see Supplementary material. In the structure of complex **7**, there is considerable disorder with the $-NMe_2$ groups and the final model used two Ti positions and several poorly defined fragments. Regardless, all non-hydrogen atoms were refined with anisotropic displacement parameters and all hydrogen atoms were placed in ideal positions and refined as riding atoms with relative isotropic displacement parameters so the overall connectivity is without question.

Coordination of the electrophile to one of the amides results in elongation of the Ti–N bond for the amine (Ti1–N2, 2.032(5) Å), when compared to the other three amide ligands (Ti1–N12, 2.018(9); Ti1–N15, 1.842(7); Ti1–N18, 1.796(9) Å). Surprisingly, complex **7** is not as active as a catalyst as $[Ti(NMe_2)_3(NHMe_2)][B(C_6F_5)_4]$ for the carboamination of internal alkynes with aldimines. Despite this discouraging result, such data suggests that the "activator" must coordinate to one of the $-NMe_2$ ligands in order to render the system active at all. In fact, changing the activator source to $[Et_3Si][B(C_6F_5)_4]$ or $[Ph_3C][B(C_6F_5)_4]$ (product not characterized) in combination with $Ti(NMe_2)_4$, aldimine, and alkyne, did result in formation of a better carboamination catalyst since conversions to the α,β-unsaturated imine product were at 42% and 37% yields, respectively, after 72 h at 130°C. Using these activators provided lower yield of product when compared to $[Ti(NMe_2)_3(NHMe_2)][B(C_6F_5)_4]$ (Table 1). The electrophiles alone, in the absence of $Ti(NMe_2)_4$, were not effective for carboamination, even when aniline was used in the reaction mixture.

2.4. Exploring the role of the labile ligand in $[Ti(NMe_2)_3(NHMe_2)][B(C_6F_5)_4]$ and 7

From the previous results, it was found that the dimethylamide ligands can undergo substitution with the ArN group of the aldimine. However, it was not clear what role the amine ligand played in the pre-catalyst complex $[Ti(NMe_2)_3(NHMe_2)][B(C_6F_5)_4]$. To investigate this, we treated the latter complex with the bulky aldimine, [2,6-^{i}Pr$_2$C$_6$H$_3$]N=CHtol, under mild conditions (25 °C, 24 h) and in the absence of the alkyne. Unfortunately the reaction resulted in a mixture of products. However, treating complex **7** with [2,6-^{i}Pr$_2$C$_6$H$_3$]N=CHtol results in mixture of products but from which were able to isolate the a metal-based complex, namely the the *N*-bound aldimine adduct $[Ti(NMe_2)_3(\kappa^1$-[2,6-^{i}Pr$_2$C$_6$H$_3$]N=CHtol)][B(C$_6$F$_5$)$_4$] (**8**) (Scheme 5). Fig. 6 displays the molecular structure of complex **8**, which possesses a cationic titanium(IV) center having an κ^1-bound imine ligand (Ti1–N2, 2.1465(13) Å) while the short N2–C3 distance of 1.289(2) Å is consistent with a relatively unperturbed imine moiety when compared to structurally similar aldimines [17]. Overall, the gross structural features of complex **8** are similar to $[Ti(NMe_2)_3(NHMe_2)][B(C_6F_5)_4]$ [9], having the basal three $-NMe_2$ ligands oriented in a propeller-type fashion, but where the amine, $HNMe_2$, has been replaced with an aldimine. This suggests that the dimethylsilylamine in complex **7** most likely serves as a labile ligand, opening a coordination site for binding of the aldimine (Scheme 3). This property could also apply to the $HNMe_2$ ligand in complex $[Ti(NMe_2)_3(NHMe_2)][B(C_6F_5)_4]$, although we were unable to isolate **8** from the complicated reaction mixture. The lability of the amine ligand explains why complex $Ti(NMe_2)_4$ must first be activated (with $[NHMe_2Ph][B(C_6F_5)_4]$ or another electrophile) in order to provide entry for the aldimine.

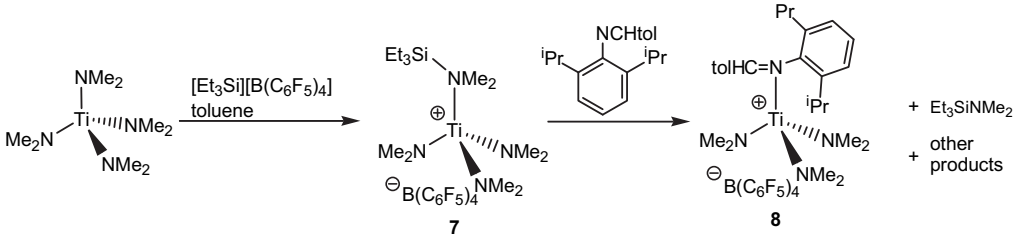

Scheme 5. Activation of $Ti(NMe_2)_4$ with $[Et_3Si][B(C_6F_5)_4]$ to form complex **7**, and preparation of aldimine **8** from **7**.

Table 1
Comparison of catalytic activities of $Ti(NMe_2)_4$ with various electrophiles for the carboamination reaction below. Reactions were carried out on a 0.25 mmol scale of aldimine using 10 mol% catalyst in C_6D_6 at 125 °C and %yield was assayed by ^1H NMR spectroscopy.

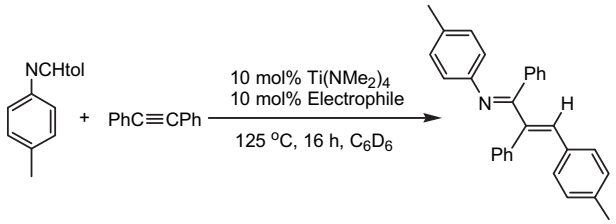

Electrophile	%yield of product
$[NHMe_2Ph][B(C_6F_5)_4]$	90
$[Et_3Si][B(C_6F_5)_4]$	42
$[Ph_3C][B(C_6F_5)_4]$	37

3. Conclusions

We have examined, reactivity wise, how the easy-to-prepare $[Ti(NMe_2)_3(NHMe_2)][B(C_6F_5)_4]$ [9] most likely performs the carboamination of alkynes with aldimines. Despite unsuccessful attempts to trap what we speculate to be the "truly active" state of the catalyst along the carboamination cycle, side products originating from stoichiometric reactions have shed some clues to reasonable intermediates formed from the pre-catalyst, $[Ti(NMe_2)_3(NHMe_2)][B(C_6F_5)_4]$. Our study suggests that the labile $HNMe_2$ ligand in $[Ti(NMe_2)_3(NHMe_2)][B(C_6F_5)_4]$ allows for coordination of the aldimine, and that formation of an imido species occurs via metathesis of the "NAr" group for two non-innocent $-NMe_2$ groups on the metal center, establishing the aldimine as the imide source. However, even though complex $[Ti(NMe_2)_3(NHMe_2)][B(C_6F_5)_4]$ is overall more active than the "Cp_2Zr=NAr" catalyst originally discovered by Bergman, such a reagent is also not atom-economical. Evidence for a neutral or cationic titanium imidos as intermediate species in the carboamination reaction has been corroborated by our ability to isolate dinuclear and catalytically active species, **2**, as well as side products such as $[Me_2N{=}CHtol][B(C_6F_5)_4]$ and $(Me_2N)_2CHtol$. However, we cannot refute the possibility of a monomer, dimer or oligomer being the active species in the catalytic cycle, due to the inherent ability of the amine to protect the titanium center as well as mask low-coordinate fragments. Finally, we have established that replacing one $-NMe_2$ group for Cp or Cp^*, or replacing $[NHMe_2Ph][B(C_6F_5)_4]$ with other activators such as Et_3Si^+ and Ph_3C^+ result in a less active carboamination catalysts when compared to $[Ti(NMe_2)_3(NHMe_2)][B(C_6F_5)_4]$.

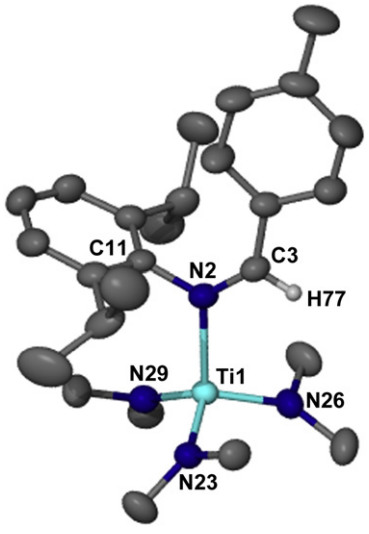

Fig. 6. Molecular structures of complexes **8** with thermal ellipsoids at the 50% probability level and with hydrogen atoms (except for the hydrogen on C3), and B $(C_6F_5)_4$ counter anion omitted for the purpose of clarity. Distances are reported in angstroms (Å) and angles in (°). Ti1–N2, 2.1465(13); Ti1–N23, 1.8670(13); Ti1–N26, 1.8550(14); Ti1–N29, 1.8666(14); N23–Ti1–N2, 110.34(5); N2–Ti1–N26, 105.29(6); N2–Ti1–N29, 110.77(6); N23–Ti1–N26, 108.62(6); N23–Ti1–N29, 110.52(6); N26–Ti1–N29, 111.16(6).

4. Experimental section

General Considerations. Unless otherwise stated, all operations were performed in an M. Braun Lab Master box under an atmosphere of purified argon or using high vacuum standard Schlenk techniques under an argon atmosphere [22]. Anhydrous *n*-hexane was purchased from Aldrich in sure-sealed reservoir (18 L) and dried by passage through two columns of activated alumina and a Q-5 column [23]. Fluorobenzene was purchased from Aldrich, degassed, and filtered through activated alumina. Deuterated benzene was purchased from Cambridge Isotope Laboratory (CIL), degassed and dried over CaH_2 then vacuum transferred to 4 Å molecular sieves. Deuterated bromobenzene was purchased from Aldrich and was dried over alumina. Celite, alumina, and 4 Å molecular sieves were activated under vacuum overnight at 200 °C. $CpTi(NMe_2)_3$ [18], $Cp^*Ti(NMe_2)_3$ [19], and $[Et_3Si][B(C_6F_5)_4]$ [21] were prepared according to the literature. $[HNMe_2Ph][B(C_6F_5)_4]$ and $[Ph_3C][B(C_6F_5)_4]$ was purchased from Boulder Scientific and dried at 60 °C for 48 h under reduced pressure to eliminate any traces of CH_2Cl_2. All the aldimines were synthesized by heating an equimolar mixture of aldehyde and corresponding aniline at 120 °C for 15–20 min. The crude aldimine product was extracted into hexanes or ether (25–50 mL). Concentration to a small volume and cooling gave crystalline solids which were filtered and dried under vacuum. All other chemicals were used as received. ^1H, ^{13}C, ^{19}F, and ^{11}B NMR spectra were recorded on Varian 400 or 300 MHz NMR spectrometers. ^1H and ^{13}C NMR are reported with reference to solvent resonances (residual C_6D_5H in C_6D_6, 7.16 ppm and 128.0 ppm; C_6D_4HBr in C_6D_5Br 7.33, 7.05, 6.97 and 131.1, 129.6, 126.4, 122.4 ppm). ^{19}F NMR chemical shifts are reported with respect to external $HOCOCF_3$ (−78.5 ppm). ^{11}B NMR spectra were reported with respect to external $BF_3{\cdot}(OEt_2)$ (0.0 ppm). X-ray diffraction data were collected on a SMART 6000 (Bruker) system under a stream of N_2 (g) at low temperatures [24,25]. Mass spectra were recorded on a ThermoFinnigan MAT 95 XP mass spectrometer.

NOTE: It is imperative that both substrates and inert atmospheres be free of moisture, oxygen, coordinating solvents (Et_2O, THF, pyridine, etc), and Cl sources (CH_2Cl_2, $CHCl_3$, CCl_4, etc). Traces of these elements will reduce the catalytic activity. It is highly recommended that substrates, solvents, and titanium precursors be freed of coordinating solvents prior to usage in catalytic reactions.

4.1. Catalytic reactions

4.1.1. Catalytic reactions using $[Ti(NMe_2)_3(NHMe_2)][B(C_6F_5)_4]$ with variance of electrophile

In a typical experiment, alkyne (PhCCPh), (0.275 mmol), tolyl substituted aldimine at C and N (0.25 mmol), dimethylanilinium tetrakis(pentafluorophenyl)borate (0.025 mmol, 10%) and $Ti(NMe)_4$ (0.025 mmol, 10%) were mixed in a J. Young NMR tube in C_6D_6 (0.8 mL) inside the glove box. The NMR tube was removed from the

glove box and was heated at 125 °C. The reaction progress was monitored by ^{1}H NMR spectroscopy. (Generally all the reactions were complete in 24 h). After the reaction was completed, the NMR tube was cooled to room temperature, the product purified by silica gel column chromatography to afford yellow α,β-unsaturated imine product. The same experiment was performed using the same amount of other electrophiles such as $[Et_3Si][B(C_6F_5)_4]$ and $[Ph_3C][B(C_6F_5)_4]$.

4.1.2. Catalytic reactions using complex **2**, $CpTi(NMe_2)_3$ and $Cp^*Ti(NMe_2)_3$

In a typical experiment, alkyne (PhCCPh), (0.275 mmol), tolyl substituted aldimine at C and N (0.25 mmol), dimethylanilinium tetrakis(pentafluorophenyl)borate (0.025 mmol, 10%) and **2**, $CpTi(NMe_2)_3$ or $Cp^*Ti(NMe_2)_3$ (0.025 mmol, 10%) were mixed in a J. Young NMR tube in C_6D_6 (0.8 mL) inside the glove box. The NMR tube was removed from the glove box and was heated at 125 °C. The reaction progress was monitored by ^{1}H NMR spectroscopy. (Generally all the reactions were complete in 24 h). After the reaction was completed, the NMR tube was cooled to room temperature, the product purified by silica gel column chromatography to afford yellow α,β-unsaturated imine product.

4.2. Isolation of the α,β-unsaturated by column chromatography

The reaction was carried out at 125 °C for 24 h as indicated above. The α,β-unsaturated imine product (Scheme 6) was purified by column chromatography (5% ether:hexanes) as a yellow solid. Recrystallization of the residue from hexane at −20 °C afforded yellow needles.

^{1}H NMR (C_6D_6, 400.12 MHz): δ 8.36 (d, J = 7.8 Hz, 2H), 7.37 (m, 4H), 7.12–7.06 (m, 4H), 7.02–6.94 (m, 3H), 6.89 (d, J = 8.2 Hz, 2H), 6.75 (d, J = 8.0 Hz, 4H), 1.96 (s, 3H), 1.94 (s, 3H). ^{13}C {H} NMR (C_6D_6, 100.62 MHz): δ 167.45, 149.34, 140.01, 138.58, 138.01, 135.91, 133.88, 133.07, 130.98, 130.84, 129.53, 129.38, 129.12, 128.93, 128.79, 128.32, 126.55, 119.72, 21.06, 20.80. One resonance is obscured by C_6D_6. HRMS CI: Calcd. for $C_{29}H_{25}N$ (M+) 387.1982, found 387.1964.

4.3. Preparation of compound **1**

$Ti(NMe_2)_4$ (104 mg, 0.463 mmol) was dissolved in C_6H_5F at room temperature. To this was added solutions of $[HNMe_2Ph][B(C_6F_5)_3]$ (371.67 mg, 0.463 mmol) and [2,6-^{i}Me$_2$C$_6$H$_3$]N=CHtol (207.17 mg, 0.926 mmol) in C_6H_5F. The solution was stirred for 3 days and filtered over Celite. The solution was layered with pentane and cooled at −35 °C, and crystals formed overnight. The product was collected in low yield (5–20%) by decanting the solution and drying the solid under vacuum.

^{1}H NMR (C_6D_6, 300.07 MHz): δ 7.53 (s, 1H), 2.94 (s, 3H), 2.91 (s, 3H), 2.16 (s, 3H). Aryl protons were obscured by solvent resonances. ^{19}F NMR (C_6D_5Br, 282.32 MHz): δ −132.6, −162.1, −166.2. Elemental Analysis. Calcd: C 49.36, H 1.70, N 1.69. Found: C 49.46, H 1.92, N 1.68.

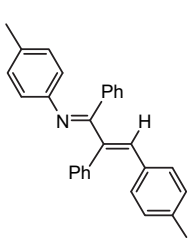

Scheme 6. α,β-Unsaturated imine using diphenylacetylene and tolyl substituted aldimine substrates.

4.4. Spectroscopic identification of $(Me_2N)_2CHtol$

To a solution of $[Ti(NMe_2)_3(NHMe_2)][B(C_6F_5)_4]$ (50–100 mg) in C_6H_5F was added an equal molar amount of [2,6-$Me_2C_6H_3$]N=CHtol. Along with several other products compound $(Me_2N)_2CHtol$ was also generated and identified by ^{1}H NMR spectroscopy as well as comparison to reported values [16]. The reaction mixture was also analyzed by high resolution chemical ionization mass spectrometry to confirm the presence of $(Me_2N)_2CHtol$. For MS-CI $(Me_2N)_2CHtol + H^+$: Calculated, 192.1621; Found, 191.1543.

4.5. Preparation of complex **2**

To a solution of $[Ti(NMe_2)_3(HNMe_2)][B(C_6F_5)_4]$ (200 mg, 0.221 mmol) in C_6H_5F was added a solution of [2,6-$Me_2C_6H_3$]N=CHtol (49.39 mg, 0.221 mmol) in C_6H_5F. The solution was stirred for 5 days and filtered over Celite. The solution was layered with pentane and cooled at −35 °C to afford crystals overnight. The product was collected in low yield (10–20%) by decanting the solution and the solid dried under vacuum.

^{1}H NMR (C_6D_6, 400.12 MHz): δ 3.25 (s, 6H), 2.66 (s, 6H), 2.64 (s, 6H), 2.12 (s, 12H), 2.00 (br, 12H). Aryl resonances were obscured by solvent. ^{19}F NMR (C_6D_5Br, 376.43 MHz): δ −132.4, −163.2, −167.1. Elemental Analysis. Calcd. (for loss of one $HNMe_2$): C 48.43, H 3.64, N 7.06. Found: C 48.23, H 3.80, N 6.37.

4.6. Preparation of complex **3**

A solution of $CpTi(NMe_2)_3$ (122.2 mg, 0.498 mmol) in C_6H_5F was cooled to −35 °C and to this was added a solution of $[HNMe_2Ph][B(C_6F_5)_3]$ in C_6H_5F. The solution was then stirred for 30 min and filtered over Celite. The solution was layered with pentane and cooled at −35 °C, and crystals formed overnight. The product was collected by filtration and dried under vacuum to yield 325.6 mg (0.350 mmol, 70.3%).

^{1}H NMR (C_6D_6, 400.12 MHz): δ 5.85 (s, 5H), 2.89, (s, 12H), 2.25 (br, 1H), 6.65 (d, J = 5.6 Hz, 6H). ^{13}C {H} NMR (C_6D_5Br, 100.62 MHz): δ 148.6 (d, J = 242.8 Hz), 138.4 (d, 258.9 Hz), 136.6 (d, 248.8 Hz), 115.3, 47.6, 40.5. One resonance was obscured by C_6D_5Br. ^{19}F NMR (C_6D_5Br, 282.32 MHz): δ −133.6, −163.6, −167.6. Elemental Analysis. Calcd: C 44.81, H 3.86, N 5.50. Found: C 44.55, H 3.87, N 5.72.

4.7. Preparation of complex **4**

A solution of $Cp^*Ti(NMe_2)_3$ (100 mg, 0.317 mmol) in C_6H_5F was cooled to −35 °C and to this solution was added a solution of $[HNMe_2Ph][B(C_6F_5)_3]$ in C_6H_5F. The solution was stirred for 30 min and then filtered over Celite. To the solution was added a few drops of hexane and red crystals formed after 12 h at box temperature (27 °C). The product was collected by decanting the solution and the solid dried under vacuum to yield 297 mg (0.298 mmol, 94.1%).

^{1}H NMR (C_6D_5Br, 400.12 MHz): δ 2.78 (s, 12H), 1.89, (s, 7H), 1.63 (s, 15H). ^{13}C {H} NMR (C_6D_5Br, 100.62 MHz): δ 148.7 (d, J = 243.1 Hz), 138.4 (d, J = 241.14 Hz), 136.6 (d, J = 241.37 Hz), 124.4, 47.0, 40.3, 11.0. One resonance was obscured by C_6D_5Br. ^{19}F NMR (C_6D_5Br, 282.32 MHz): δ −133.3, −165.9, −168.2. Elemental Analysis. Calcd: C 48.27, H 3.44, N 4.22. Found: C 48.33, H 3.53, N 4.09.

4.8. Preparation of complex **5**

A solution of **3** (67.4 mg, 0.073 mmol) in C_6H_5F was added to a J-Young tube and to this solution was added 12.9 mg (0.073 mmol) of 2,6-diisopropyl aniline. The reaction was heated at 110 °C for 72 h and the mixture filtered through Celite. The solution was layered with pentane and after 12 h at −35 °C crystals were grown and

collected by decanting the solution and drying the solid under vacuum to yield 44.5 mg (0.041 mmol, 58%) of the desired product.

^{1}H NMR (C_6D_5Br, 400.12 MHz): δ 6.08 (s, 5H), 3.04 (sept, J = 6.8 Hz, 2H), 2.99, (br, 2H), 2.30 (br, 6H), 2.22 (br, 6H), 1.14 (6, J = 7.1 Hz, 12 H). Aryl protons were obscured by solvent. ^{19}F NMR (C_6D_5Br, 282.32 MHz): δ −132.7, −162.2, −166.3. Elemental Analysis Calcd. (with one C_6H_5F included): C 53.10, H 3.58, N 3.64. Found: C 52.99, H 3.50, N 4.08.

4.9. Preparation of complex **6**

A solution of **4** (65.1 mg, 0.065 mmol) in C_6H_5F was added to a J-Young tube. To this was added 11.5 mg (0.098 mmol) of 2,6-diisopropyl aniline. The reaction was heated at 110 °C for 72 h. The solution was then filtered through Celite and layered with pentane. After 12 h at −35 °C crystals were grown and then collected by filtration and dried under vacuum to yield 25.7 mg (0.023 mmol, 35%) of the desired product.

^{1}H NMR (C_6D_5Br, 400.12 MHz): δ 6.99 (d, J = 6.7 Hz, 2H), 6.87 (t, J = 6.7 Hz, 1H), 2.67 (sept, J = 6.8 Hz, 2H), 2.61 (br, 6H), 2.49 (br, 2H), 2.33 (br, 6h), 1.74 (s, 15H), 1.12 (d, J = 6.8 Hz, 12H). ^{13}C {H} NMR (C_6D_5Br, 100.62 MHz): δ 138.2 (d, J = 239.8 Hz), 128.0 (d, J = 247.6 Hz), 126.1 (d, J = 245.0 Hz), 114.1, 110.9, 110.4, 104.8, 104.6, 36.6, 29.8, 25.8, 0.5. ^{19}F NMR (C_6D_5Br, 282.32 MHz): δ −131.9, −162.1, −166.1. Elemental Analysis. Calculated: C 53.26, H 4.11, N 3.72. Found: C 52.36, H 3.92, N 4.06.

4.10. Preparation of complex **7**

A solution of $Ti(NMe_2)_4$ (100 mg, 0.446 mmol) in C_6H_5F was cooled to −35 °C. To this was added a solution of $[Et_3Si][B(C_6F_5)_3]$ in C_6H_5F. The mixture was stirred for 15 min and filtered over Celite. The solution was layered with pentane and cooled at −35 °C, and crystals formed overnight. The product was collected by decantation and dried under vacuum to yield 393 mg (0.386 mmol, 86.5%).

^{1}H NMR (C_6D_6, 300.07 MHz): δ 2.95 (s, 3H), 2.89 (s, 24H), 2.15 (s, 3H), 0.80 (t, J = 7.7 Hz, 9H), 0.57 (q, J = 7.9 Hz, 6H). ^{11}B NMR (C_6D_5Br, 128.37 MHz): δ −16.3. ^{19}F NMR (C_6D_5Br, 282.32 MHz): δ −131.9, −162.2, −166.1. Elemental Analysis. Calcd: C 44.81, H 3.86, N 5.50. Found: C 44.55, H 3.87, N 5.72.

4.11. Preparation of complex **8**

To a solution of **7** (171 mg, 0.167 mmol) in C_6H_5F was added a solution of [2,6-^{i}Pr$_2$C$_6$H$_3$]N=CHtol (46.92 mg, 0.167 mmol) in C_6H_5F. The solution was stirred for 20 h and filtered through Celite. The solution was then layered with pentane and cooled at −35 °C, and crystals formed overnight. The product was collected by decantation and dried under vacuum.

^{1}H NMR (C_6D_6, 400.12 MHz): δ 8.12 (s, 1H), 7.07 (dd, J = 8.42, 16.24 Hz, 1H), 6.94 (d, 7,79 Hz, 2H), 6.57 (q, 8.45 Hz, 4H), 2.79 (s, 18H), 2.20 (sept, 6.73 Hz, 2H). 1.77 (s, 3H), 0.81 (d, 6.80 Hz, 6H), 0.52 (d, 6.74 Hz, 6H). ^{11}B NMR (C_6D_5Br, 128.37 MHz): δ −16.3. ^{13}C {H} NMR (C_6D_5Br, 100.62 MHz): δ 173.8, 149.6, 148.7 (d, 235.62 Hz), 138.8, 138.5 (d, 243.76 Hz), 138.3, 136.6 (d, 241.53 Hz), 134.0, 130.5, 126.5, 125.8, 43.7, 43.1, 28.8, 24.3, 23.1, 21.7. Two aryl resonances were obscured by C_6D_5Br. ^{19}F NMR (C_6D_5Br, 376.43 MHz): δ −133.4, −163.9, −167.7. Elemental Analysis. Calcd: C 52.75, H 3.81, N 4.92. Found: C 52.57, H 3.87, N 4.74.

4.12. X-ray crystallographic data

Single crystals of **1** were grown from a fluorobenzene/hexane-layered solution at room temperature under an N_2 atmosphere. Crystal data for $C_{34}H_{14}BF_{20}N$, **1**: M = 827.27, Monoclinic, space group P2(1)/c, a = 15.311(7) Å, b = 10.607(5) Å, c = 19.260(9) Å, β = 92.558 (11)°, $\alpha = \gamma$ = 90°, U = 3125(2) Å^3, Z = 4, D_c = 1.759 g cm^{-3}, λ (MoKα) = 0.71073 mm^{-1}, T = 173(2) K, Bruker SMART 6000, total reflections 38,916, unique reflections $F > 4\sigma(F)$, 7172, observed reflections 3194 (R_{int} = 0.1108). The structure was solved using SHELXS-97 and refined with SHELXL-97. A direct-method solution was calculated which provided most non-hydrogen atoms from the E-map. Full-matrix least squares/difference Fourier cycles were performed which located the remaining non-hydrogen atoms. All non-hydrogen atoms were refined with anisotropic displacement parameters. Although the anion was well defined and ordered it was apparent that there was a disorder with the $C_{10}H_{14}N$ cation. Examination of residuals indicated that the molecule is "flipped" about the long axis about 20% or the time. The SHELX "SAME" command was used to refine the secondary structure. All hydrogen atoms were placed in ideal positions and refined as riding atoms with relative isotropic displacement parameters. GOF = 0.732 and the final refinement converged at $R(F)$ = 0.0366 (observed data) and wR (F^2) = 0.0617 (refinement data).

Single crystals of **2** were grown from a fluorobenzene/hexane-layered solution at room temperature under an N_2 atmosphere. Crystal data for $C_{68}H_{65}BF_{23}N_7Ti_2$, **2**: M = 1523.88, Triclinic, space group P−1, a = 12.2372(13) Å, b = 16.6642(18) Å, c = 17.4838(19) Å, α = 83.185(3)°, β = 71.840(4)°, γ = 83.243(3)°, U = 3351.5(6) Å^3, Z = 2, D_c = 1.510 g cm^{-3}, λ(MoKα) = 0.71073 mm^{-1}, T = 123(2) K, Bruker SMART 6000, total reflections 76,283, unique reflections $F > 4\sigma(F)$, 15,458 observed reflections 9935 (R_{int} = 0.0861). The structure was solved using SHELXS-97 and refined with SHELXL-97. A direct-method solution was calculated which provided most non-hydrogen atoms from the E-map. Full-matrix least squares/difference Fourier cycles were performed which located the remaining non-hydrogen atoms. All non-hydrogen atoms were refined with anisotropic displacement parameters. In addition to the Ti dimer and anion, there are four C_6H_5F solvent molecules present, all disordered and two lying on centers of inversion. All hydrogen atoms were placed in ideal positions and refined as riding atoms with relative isotropic displacement parameters. GOF = 1.035 and the final refinement converged at $R(F)$ = 0.0669 (observed data) and $wR(F^2)$ = 0.1919 (refinement data).

Single crystals of **3** were grown from a fluorobenzene/hexane-layered solution at room temperature under an N_2 atmosphere. Crystal data for $C_{41}H_{29}BF_{21}N_3Ti$, **3**: M = 1021.38, Monoclinic, space group P2(1)/c, a = 12.027(2) Å, b = 21.591(4) Å, c = 17.203(3) Å, α = 90°, β = 108.993(5)°, γ = 90°, U = 4223.9(14) Å^3, Z = 4, D_c = 1.606 g cm^{-3}, λ(MoKα) = 0.71073 mm^{-1}, T = 123(2) K, Bruker SMART 6000, total reflections 54,918, unique reflections $F > 4\sigma(F)$, 9741 observed reflections 5971 (R_{int} = 0.0673). The structure was solved using SHELXS-97 and refined with SHELXL-97. A direct-method solution was calculated which provided most non-hydrogen atoms from the E-map. Full-matrix least squares/difference Fourier cycles were performed which located the remaining non-hydrogen atoms. One FC_6H_5 solvent molecule was found in the asymmetric unit. All non-hydrogen atoms were refined with anisotropic displacement parameters. All hydrogen atoms were placed in ideal positions and refined as riding atoms with relative isotropic displacement parameters. GOF = 0.870 and the final refinement converged at $R(F)$ = 0.0352 (observed data) and $wR(F^2)$ = 0.0799 (refinement data).

Single crystals of **4** were grown from a fluorobenzene/hexane-layered solution at room temperature under an N_2 atmosphere. Crystal data for $C_{40}H_{34}BF_{20}N_3Ti$, **4**: M = 995.41, Triclinic, space group P−1, a = 14.7239(8) Å, b = 15.7062(9) Å, c = 19.0241(11) Å, α = 105.504(2)°, β = 107.322(2)°, γ = 91.870(2)°, U = 4016.9(4) Å^3, Z = 4, D_c = 1.646 g cm^{-3}, λ(MoKα) = 0.71073 mm^{-1}, T = 133(2) K, Bruker SMART 6000, total reflections 39,538, unique reflections $F > 4\sigma(F)$, 23,272 observed reflections 11,556 (R_{int} = 0.0512). The

structure was solved using SHELXS-97 and refined with SHELXL-97. A direct-method solution was calculated which provided most non-hydrogen atoms from the E-map. Full-matrix least squares/difference Fourier cycles were performed which located the remaining non-hydrogen atoms. The structure was found as proposed with two independent molecules per asymmetric unit. All non-hydrogen atoms were refined with anisotropic displacement parameters. All hydrogen atoms were placed in ideal positions and refined as riding atoms with relative isotropic displacement parameters. GOF = 0.756 and the final refinement converged at $R(F) = 0.0447$ (observed data) and $wR(F^2) = 0.0848$ (refinement data).

Single crystals of **6** were grown from a fluorobenzene/hexane-layered solution at room temperature under an N_2 atmosphere. Crystal data for $C_{50}H_{46}BF_{20}N_3Ti$, **6**: $M = 1127.61$, Monoclinic, space group P2(1)/n, $a = 17.654(2)$ Å, $b = 13.7175(17)$ Å, $c = 21.887(3)$ Å, $\alpha = \gamma = 90°$, $\beta = 109.354(3)°$, $U = 5000.9(11)$ Å, $Z = 4$, $D_c = 1.498$ g cm^{-3}, λ (MoKα) = 0.71073 mm^{-1}, $T = 125(2)$ K, Bruker SMART 6000, total reflections 38,290, unique reflections $F > 4\sigma(F)$, 11,489 observed reflections 6443 ($R_{int} = 0.0682$). The structure was solved using SHELXS-97 and refined with SHELXL-97. A direct-method solution was calculated which provided most non-hydrogen atoms from the E-map. Full-matrix least squares/difference Fourier cycles were performed which located the remaining non-hydrogen atoms. All non-hydrogen atoms were refined with anisotropic displacement parameters. All hydrogen atoms were placed in ideal positions and refined as riding atoms with relative isotropic displacement parameters. GOF = 0.825 and the final refinement converged at $R(F) = 0.0351$ (observed data) and $wR(F^2) = 0.0783$ (refinement data).

Single crystals of **7** were grown from a fluorobenzene/hexane-layered solution at room temperature under an N_2 atmosphere. Crystal data for $C_{38}H_{39}BF_{20}N_4SiTi$, **7**: $M = 1018.54$, Orthorhombic, space group Pbca, $a = 16.802(8)$ Å, $b = 20.973(10)$ Å, $c = 24.050(11)$ Å, $\alpha = \beta = \gamma = 90°$, $U = 8475(7)$ Å^3, $Z = 8$, $D_c = 1.598$ g•cm^{-3}, λ (MoKα) = 0.71073 mm^{-1}, $T = 123(2)$ K, Bruker SMART 6000, total reflections 38,089, unique reflections $F > 4\sigma(F)$, 9745 observed reflections 4703 ($R_{int} = 0.0822$). The structure was solved using SHELXS-97 and refined with SHELXL-97. A direct-method solution was calculated which provided most non-hydrogen atoms from the E-map. Full-matrix least squares/difference Fourier cycles were performed which located the remaining non-hydrogen atoms. There is considerable disorder with the $-NMe_2$ groups. The final model used two Ti positions and several poorly defined fragments. All non-hydrogen atoms were refined with anisotropic displacement parameters. All hydrogen atoms were placed in ideal positions and refined as riding atoms with relative isotropic displacement parameters. GOF = 0.905 and the final refinement converged at $R(F) = 0.0653$ (observed data) and $wR(F^2) = 0.2124$ (refinement data).

Single crystals of **8** were grown from a fluorobenzene/hexane-layered solution at room temperature under an N_2 atmosphere. Crystal data for $C_{50}H_{43}BF_{20}N_4Ti$, **8**: $M = 1138.59$, Triclinic, space group P−1, $a = 10.0164(14)$ Å, $b = 15.180(2)$ Å, $c = 16.942(3)$ Å, $\alpha = 95.485(4)°$, $\beta = 99.275(4)°$, $\gamma = 94.871(4)°$, $U = 2517.4(7)$ Å^3, $Z = 2$, $D_c = 1.502$ g cm^{-3}, λ(MoKα) = 0.71073 mm^{-1}, $T = 122(2)$ K, Bruker SMART 6000, total reflections 69,434, unique reflections $F > 4\sigma(F)$, 14,742 observed reflections 9778 ($R_{int} = 0.0588$). The structure was solved using SHELXS-97 and refined with SHELXL-97. A direct-method solution was calculated which provided most non-hydrogen atoms from the E-map. Full-matrix least squares/difference Fourier cycles were performed which located the remaining non-hydrogen atoms. All non-hydrogen atoms were refined with anisotropic displacement parameters. All hydrogen atoms were placed in ideal positions and refined as riding atoms with relative isotropic displacement parameters. GOF = 0.966 and the final refinement converged at $R(F) = 0.0447$ (observed data) and $wR(F^2) = 0.1286$ (refinement data).

Acknowledgements

We thank Dr. Aneetha Halikhedkar for insightful discussions and Indiana University-Bloomington, and the Chemical Sciences, Geosciences and Biosciences Division, Office of Basic Energy Science, Office of Science, U.S. Department of Energy (No. DE-FG02-07ER15893) for financial support of this research.

Appendix A. Supplementary material

CCDC 786995–787001 contain the supplementary crystallographic data for this paper. These data can be obtained free of charge from The Cambridge Crystallographic Data Center via www.ccdc.cam.ac.uk/data_request/cif.

References

[1] R.T. Ruck, R.G. Bergman, Organometallics 23 (2004) 2231.
[2] R.T. Ruck, R.L. Zuckermann, S.W. Krska, R.G. Bergman, Angew. Chem. Int. Ed. 43 (2004) 5372.
[3] (a) S.W. Krska, R.L. Zuckerman, R.G. Bergman, J. Am. Chem. Soc. 120 (1998) 11828; (b) K.E. Meyer, P.J. Walsh, R.G. Bergman, J. Am. Chem. Soc. 116 (1994) 2669.
[4] A.R. Fout, U.J. Kilgore, D.J. Mindiola, Chem. Eur. J. 13 (2007) 9428.
[5] D.J. Mindiola, Comments Inorg. Chem. 29 (2008) 73.
[6] (a) F. Basuli, J.C. Huffman, D.J. Mindiola, Inorg. Chem. 42 (2003) 8003; (b) F. Basuli, B.C. Bailey, J.C. Huffman, D.J. Mindiola, Chem. Commun. (2003) 1554.
[7] F. Basuli, H. Annetha, J.C. Huffman, D.J. Mindiola, J. Am. Chem. Soc. 127 (2005) 17992.
[8] F. Basuli, R.L. Clark, B.C. Bailey, D. Brown, J.C. Huffman, D.J. Mindiola, Chem. Commun. (2005) 2250.
[9] H. Aneetha, F. Basuli, J. Bollinger, J.C. Huffman, D.J. Mindiola, Organometallics 25 (2006) 2402.
[10] A.L. Odom, Dalton Trans. (2005) 225.
[11] (a) Y. Shi, J.T. Ciszewski, A.L. Odom, Organometallics 20 (2001) 3967; (b) Y. Shi, J.T. Ciszewski, A.L. Odom, Organometallics 21 (2002) 5148.
[12] J.A. Bexrud, J.D. Beard, D.C. Leitch, L.L. Schafer, Org. Lett. 7 (2005) 1959.
[13] N. Hazari, P. Mountford, Acc. Chem. Res. 38 (2005) 839.
[14] (a) D.E. Wigley, Prog. Inorg. Chem. 42 (1994) 239; (b) W.A. Nugent, J.M. Mayer, Metal-Ligand Multiple Bonds. John Wiley & Sons, New York, 1988; (c) L.H. Gade, P. Mountford, Coord. Chem. Rev. 216 (2001) 65; (d) A.P. Duncan, R.G. Bergman, Chem. Rec. 2 (2002) 431; (e) W.A. Nugent, B.L. Haymore, Coord. Chem. Rev. 31 (1980) 123.
[15]. P. Gomez-Sal, A. Martin, M. Mena, M.C. Morales, C. Santamaria, Chem. Commun. (1999) 1839.
[16] H. Boehme, M. Haake, G. Auterhoff, Archiv der Pharmazie 305 (1972) 10.
[17] (a) 1.250(15) Å has been reported for dialdimine, 1,2-[[2,6-^{i}Pr$_2$C$_6$H$_3$]N=CH]$_2$C$_6$H$_4$. J.M. Chitanda, D.E. Prokopchuk, J.W. Quail, S.R. Foley Organometallics 27 (2008) 2337; (b) 1.274 Å for 2,6-[[2,6-^{i}Pr$_2$C$_6$H$_3$]N=C(CH$_3$)]2C$_6$H$_4$. S. Nuckel, P. Burger Organometallics 19 (2000) 3305
[18] G. Chandra, M.F. Lappart, J. Chem. Soc. A (1968) 1940.
[19] A. Martin, M. Mena, C. Yélamos, R. Sarrano, J. Organomet. Chem. 467 (1994) 79.
[20] For some recent reviews and manuscripts. (a) K. Weitershaus, B.D. Ward, R. Kubiak, C. Müller, H. Wadepohl, S. Doye, L.H. Gade, Dalton Trans. (2009) 4586; (b) P.W. Roesky, T.E. Müller, Angew. Chem., Int. Ed. 42 (2003) 2708; (c) F. Pohlki, S. Doye, Chem. Soc. Rev. 32 (2003) 104; (d) I. Bytschkov, S. Doye, Eur. J. Org. Chem. (2003) 935; (e) J.F. Hartwig, Pure Appl. Chem. 76 (2004) 507; (f) F. Alonso, I.P. Beletskaya, M. Yus, Chem. Rev. 104 (2004) 3079; (g) S. Doye, Synlett (2004) 1653; (h) K.C. Hultzsch, Adv. Synth. Catal. 347 (2005) 367; (i) K.C. Hultzsch, Org. Biomol. Chem. 3 (2005) 1819; (j) R. Severin, S. Doye, Chem. Soc. Rev. 36 (2007) 1407; (k) T.E. Müller, K.C. Hultzsch, M. Yus, F. Foubelo, M. Tada, Chem. Rev. 108 (2008) 3795; (l) J.-J. Brunet, N.-C. Rodriguez-Zubiri, Eur. J. Inorg. Chem. (2007) 4711; (m) P.L. McGrane, M. Jensen, T. Livinghouse, J. Am. Chem. Soc. 114 (1992) 5459; (n) J.S. Johnson, R.G. Bergman, J. Am. Chem. Soc. 123 (2001) 2923.
[21] (a) J.B. Lambert, S. Zhang, S.M. Ciro, Organometallics 13 (1994) 2430; (b) V.J. Scott, R. Celenligil-Cetin, O.V. Ozerov, J. Am. Chem. Soc. 127 (2005) 2852.
[22] For a general description of the equipment and techniques used in carrying out this chemistry see: B.J. Burger, J.E. Bercaw, in: A.L. Wayda, M.Y. Darensbourg (Eds.), Experimental Organometallic Chemistry, ACS Symposium Series, 357, American Chemical Society, Washington D.C., 1987, pp. 79–98.
[23] A.B. Pangborn, M.A. Giardello, R.H. Grubbs, R.K. Rosen, F.J. Timmers, Organometallics 15 (1996) 1518.
[24] SAINT 6.1, Bruker Analytical X-Ray Systems, Madison, WI.
[25] SHELXTL-Plus V5.10, Bruker Analytical X-Ray Systems, Madison, WI.